DOI: 10.1002/chem.200501499

Electrocarboxylation of Benzyl Halides through Redox Catalysis on the Preparative Scale

Onofrio Scialdone,*[a] Alessandro Galia,[a] Giuseppe Silvestri,[a] Christian Amatore,*[b] Laurent Thouin,[b] and Jean-Noel Verpeaux[b]

Abstract: The electrocarboxylation of benzyl halides to the corresponding carboxylic acids through homogeneous charge-transfer catalysis was investigated both theoretically and experimentally to determine the influence of the operative parameters on the yield of the process and on the catalyst consumption. Theoretical considerations, based on fast kinetics of redox catalysis, were confirmed by the electrocarboxylation of 1-phenyl-1-chloroethane catalyzed by 1,3-benzenedicarboxylic acid dimethyl ester performed at a carbon cathode under different operative conditions. We obtained high yields of the target carboxylic acid and experienced a low catalyst consumption by operating with optimized $[RX]^{bulk}/[CO_2]^{bulk}$ and $[RX]^{bulk}$/[catalyst] ratios.

Keywords: benzyl halides · carbon dioxide · carboxylation · electrochemistry · homogeneous catalysis

Introduction

Carbon dioxide is a central and inexpensive building block in organic synthesis. It undergoes facile reaction with carbanions or procarbanions, as in Grignard reactions, in order to add an extra carbon unit to an organic skeleton while maintaining an open functionalization. This is also a very convenient way to introduce a carboxylic function onto an organic carbon center. On the other hand, electrochemical reduction of organic halides or pseudohalides is a very convenient and cheap way to stoichiometrically generate carbanions or procarbanions. Hence, many efforts have been devoted to the mechanistic and preparative aspects of electrocarboxylation of organic halides and pseudohalides, some of which have led to the set up of pilot plants for industrial application, particularly for the production of anti-inflammatory drugs.[1–18]

[a] Dr. O. Scialdone, Dr. A. Galia, Prof. Dr. G. Silvestri
Dipartimento di Ingegneria Chimica
dei Processi e dei Materiali
Viale delle Scienze 90128 Palermo (Italy)
Fax: (+33) 09-1656-7280
E-mail: scialdone@dicpm.unipa.it

[b] Prof. Dr. C. Amatore, Dr. L. Thouin, Prof. J.-N. Verpeaux
Ecole Normale Supérieure, Département de Chimie
UMR CNRS-ENS-UPMC 8640 "PASTEUR"
24 rue Lhomond, 75231 Paris Cedex 05 (France)
Fax: (+33) 1-4432-3863
E-mail: christian.amatore@ens.fr

Ideally, the electrocarboxylation of organic halides can be shown by the simple following sequence:

$$RX + e^- \rightarrow RX^{\cdot -} \quad (1)$$

$$RX^{\cdot -} \rightarrow R^{\cdot} + X^- \quad (2)$$

$$R^{\cdot} + e^- \rightarrow R^- \quad (3)$$

$$R^- + CO_2 \rightarrow RCOO^- \quad (4)$$

where RX is the organic halide or pseudohalide (note that steps (1) and (2) may be concerted so that the anion radical $RX^{\cdot -}$ may not exist). In fact, this sequence uses the two-electron reduction of the carbon-leaving-group bond to invert the polarity of the carbon center, so that the analogy with the textbook mechanism of Grignard carboxylations is almost total. However, under some circumstances (for example, when the carbon–halogen bond is not activated enough by the proximity of a π^* system, or because the organic moiety bears electron-donating groups, or when the halide is a poor leaving group such as a chloride etc.), this reduction may require potentials that are too negative, making it less attractive from an industrial point of view, and may even lead to several byproducts resulting from the fact that carbon dioxide may be reduced concurrently:

$$CO_2 + e^- \rightarrow CO_2^{\cdot -} \rightarrow \text{etc.} \quad (5)$$

For direct processes, it has been recently shown in microscale syntheses that the use of a silver cathode allows operation at a more positive potential even if the long term activity of the electrode surface at the preparative scale has still to be tested.[17,18] Two catalytic routes have been proposed for performing the electrocarboxylation at a much less-negative electrode potential than that required for RX reduction. One consists of using a transition-metal catalyst (TM^{II}) where the process takes place at its facile overall two-electron reduction potential. This generates a zerovalent metal center (TM^0) that undergoes oxidative addition to the organic halide or pseudohalide to generate an organometal ($R\text{-}TM^{II}X$) species reducible at this potential. Reduction of this species generally occurs at potentials much less negative than that of the parent organic halide due to the activation by the metal(II) center producing an organometal, RTM^I [Eq. (8)] or an organometal(0) anion [Eq. (9)], depending on the nature of the metal catalyst and of its ligands.

$$TM^{II} + 2e^- \rightarrow TM^0 \quad (6)$$

$$TM^0 + RX \rightarrow R\text{-}TM^{II}X \quad (7)$$

$$R\text{-}TM^{II}X + e^- \rightarrow R\text{-}TM^{I} + X^- \quad (8)$$

$$R\text{-}TM^{II}X + 2e^- \rightarrow R\text{-}TM^{0-} + X^- \quad (9)$$

In the first case, for example, with $[NiCl_2(dppe)]$ as the catalyst, CO_2 undergoes oxidative addition to the organometal(I) center to yield a $R\text{-}TM^{III}(CO_2)$ species that undergoes a facile reductive elimination of the carboxylate anion to generate a metal(I) moiety that is reduced back to the zerovalent form so that a new cycle may proceed [Eqs. (10–12)].

$$R\text{-}TM^{I} + CO_2 \rightarrow R\text{-}TM^{III}(CO_2) \quad (10)$$

$$R\text{-}TM^{III}(CO_2) \rightarrow RCO_2^- + TM^{I} \quad (11)$$

$$TM^{I} + e^- \rightarrow TM^0 \quad (12)$$

In the second case, for example, with $[PdCl_2(PPh_3)_2]$ as the catalyst, the anionic organometal(0) cleaves off reversibly to produce the organic anion R^- [Eq. (13)],

$$R\text{-}TM^{0-} \rightleftharpoons R^- + TM^{II} \quad (\Delta G^0 \gg 0) \quad (13)$$

that reacts with CO_2 [Eq. (4)], and a metal(II) species that is reduced back to the zerovalent metal species [Eq. (6)] closing the catalytic cycle. Both routes are fully documented in the literature and their mechanisms duly established.[9–15] They are extremely useful routes since the metal-center participation almost avoids the formation of byproducts. Indeed, in the first case the reactive radical $R^\bullet$ and anion R^- are not produced, while in the second case $R^\bullet$ is not produced and R^- is "protected" under the $R\text{-}TM^{0-}$ form due to the large endergonicity of the equilibrium shown in Equation (13) so that it can react only with the strongest electrophiles (namely CO_2). However, the main disadvantage of these routes for use in large-scale electrolysis is that they often require the use of poorly coordinating solvents, that is, of poorly conducting or unusual electrolytes that impose large ohmic-drop losses in a large cell. At the laboratory scale where the cell energetics and production rate are not a problem, this is easily compensated by large cell tensions and low current densities but this is not a viable solution at the larger preparative-scale except for the electrosynthesis of products with extremely high added value.

The second alternative to bypass the difficult RX reduction consists of using redox catalysis. Thus, the reduction of RX can be performed at the much less-negative one-electron reversible reduction potential [Eq. (14)] of an adequate redox mediator M that delivers the electron to the RX species through an homogeneous electron transfer when $RX^{\bullet -}$ is present [Eq. (15)], or for a concerted bond-breaking RX reduction [Eq. (16)].

$$M + e^- \rightarrow M^{\bullet -} \quad (14)$$

$$M^{\bullet -} + RX \rightleftharpoons M + RX^{\bullet -} (\rightarrow R^\bullet + X^-) \quad (15)$$

$$M^{\bullet -} + RX \rightarrow M + R^\bullet + X^- \quad (16)$$

Although the redox mediator M is reduced at much more positive potentials than RX, the reactions shown in Equations (15) or (16) are kinetically displaced towards the formation of $R^\bullet$ due to the irreversibility of the cleavage of the carbon–halogen bond. The above sequence is then completed by the reduction of $R^\bullet$ into R^- [Eq. (17)] that then reacts with CO_2 to yield the organic carboxylate [Eq. (4)], so that the desired product is electrogenerated at the reduction potential of the redox mediator catalyst.

$$M^{\bullet -} + R^\bullet \rightleftharpoons M + R^- \quad (17)$$

From a preparative point of view, this alternative is a priori excellent. Indeed, the cell can be operated at a much less-negative potential than that required for the direct reduction of RX. Importantly, the reaction can take place in polar solvents so that ohmic-drop energy losses are minimized and significant current densities can be applied. Also, the anionic carboxylate is easily separated from the generally poorly water-soluble redox mediator. Furthermore, the fact that the electrode experiences only a reduction of the extremely chemically stable $M/M^{\bullet -}$ redox couple prevents the electrode deactivation that often occurs when direct reduction of RX is performed on the preparative scale with lost-cost cathode material.[6,7] Finally and very importantly, the cathodic process is compatible with the use of a sacrificial anode so that the whole cell can be operated in a single-compartment mode, that is, without the requirement for a diaphragm that would increase the ohmic-drop losses. In this respect, we should note that the operation in the single-compartment mode with a sacrificial anode (Al, Mg) may even be extremely beneficial since the small cations Met^{n+} gener-

ated at the anode may readily complex the carboxylate formed.

$$\mathrm{Met(anode)} - n\,\mathrm{e}^- \rightleftharpoons \mathrm{Met}^{n+} \quad (18)$$

$$\mathrm{Met}^{n+} + n\,\mathrm{RCO_2}^- \rightleftharpoons \mathrm{Met(RCO_2)_n} \quad (19)$$

preventing the possible esterification of the parent RX.[19]

$$\mathrm{RX} + \mathrm{RCO_2}^- \not\rightarrow \mathrm{RCOOR} + \mathrm{X}^- \quad (20)$$

Presumably, this is also true for the coordination of R^- so that this strong base is kinetically stabilized and able to react almost exclusively with carbon dioxide instead of being partially protonated in the medium. In this context, it is worth emphasizing that the operation of the cell in a single-compartment mode with a sacrificial anode promotes the electrogeneration of ions proportionally to the charge passed. These can sustain the current flow in the cell so that there is usually no need to operate in the presence of a high concentration of added supporting electrolyte in batch cells.

Considering all these advantages brought about by redox catalysis, one may wonder why the method is not more widespread since it is applicable with the same benefits even in cases where a direct reduction would be feasible. A first answer could be that if the RX reduction can be catalyzed by the redox mediator, the reduction of CO_2 must also be catalyzed. In fact this is partially true, since the homogeneous reduction of CO_2 may indeed occur.

$$\mathrm{M}^{\cdot-} + \mathrm{CO_2} \rightleftharpoons \mathrm{M} + \mathrm{CO_2}^{\cdot-} \quad (21)$$

However, the reaction proceeds at a much slower rate than that of RX because the uphill equilibrium [Eq. (21)] is driven now by the slower bimolecular duplication of $CO_2^{\cdot-}$ to produce oxalate:

$$2\,\mathrm{CO_2}^{\cdot-} \rightarrow \mathrm{C_2O_4}^{2-} \quad (22)$$

Furthermore, the forward homogeneous electron-transfer [Eq. (21)] rate constant k_{21} has been shown to have a much stronger dependence on the standard potential E^0_M of the redox mediator, than that of the forward rate constant k_{ET} of the homogeneous reduction shown in Equations (15) or (16);[7,20] thus $\partial(\log k_{21})/\partial(-E^0_M) = 1/60 - 1/120$ per mV while, $\partial(\log k_{ET})/\partial(-E^0_M) = 1/200$ per mV. Thus, selecting a redox mediator with a sufficiently positive redox potential prevents the electron-transfer activation of CO_2.[7]

Therefore, the above question reflects more profound difficulties. In fact, most of these difficulties are an inherent part of redox catalysis itself and manifest themselves under preparative-scale conditions. In our view, this is the main reason why, despite the immense theoretical advantages from an industrial point of view, redox catalysis based on organic mediators has seldom been applied on the preparative scale and has remained restricted to the much smaller laboratory scale or to splendid kinetic analyses.

It is important to realize that in preparative conditions, as the chemical kinetics of the charge transfer is fast with respect to the diffusion rate, the concentration profiles of the mediator and substrate are fixed exclusively by the two diffusion rates of the two reacting species. Hence, the diffusion layer separates into two domains where pure diffusion takes place and the concentration profiles are mainly linear, the limit between each zone being set by the condition of identical fluxes for each reacting species.[21] More precisely, it has been demonstrated by mapping concentration profiles within the diffusion layer of an electrode,[21] that if a sufficiently fast charge transfer is involved, $M^{\cdot-}$ and the substrate RX may exist simultaneously only within a thin strip of solution of an extremely small thickness (that we will call the reaction layer in the following) if compared with that δ of the diffusion layer located at distance μ from the electrode surface as shown in Figure 1a and b. Hence, reactions involving

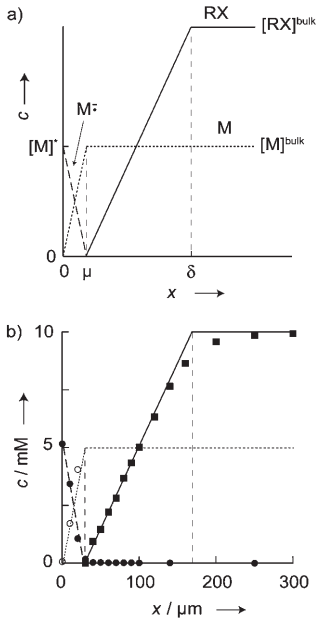

Figure 1. a) Theoretical concentration profiles during the catalytic reduction of the substrate RX by the radical anion $M^{\cdot-}$ of the mediator M. Note in this case that $[M]^* = [M]^{bulk}$ (see Eq. (24) with $E \gg E^0_M$). b) Concentration profiles established experimentally during the catalytic reduction of 10 mM iodobenzene by 5 mM benzophenone in 0.1 M nBu$_4$NBF$_4$/DMF: benzophenone (○), benzophenone radical anion (●), and iodobenzene(■). Adapted from ref. [21].

R^- occur in a very thin strip of solution where very low concentrations of R^- exist while in the portion of the diffusion layer between the electrode surface and the reaction layer no carboxylation reaction occurs and $M^{\cdot-}$ is involved only in competitive reactions thus leading to the destruction of a small but non-negligible fraction of the redox mediator at each cycle.

In particular μ, as shown in Equation (23), does not depend on kinetics but only on the ratio of the bulk concentrations of each species ($[RX]^{bulk}$ and $[M]^{bulk}$) multiplied by

their diffusion coefficients (D_{RX} and D_M) and on the working potential E.

$$\mu = \frac{\delta}{1+\frac{2D_{RX}[RX]^{bulk}}{D_M[M]^*}} \quad (23)$$

where

$$[M]^* = \frac{[M]^{bulk}}{1+\exp\left(\frac{F(E-E^0_M)}{RT}\right)} \quad (24)$$

in which D_M and D_{RX} are the diffusion coefficients, and $[M]^{bulk}$ and $[RX]^{bulk}$ are the bulk concentrations of M and RX, and Faraday constant F.

This particular structuring of the diffusion layer can lead to very important consequences concerning the selectivity of the process and the stability of the mediator. In the following, we will investigate the impact of this structural layer on the process and propose strategies for optimizing the process in the frame of electrocarboxylation, yet most of the presented analysis, strategies, and conclusions are easily transposable to a wider variety of electropreparative processes.

Results and Discussion

Theoretical discussion

The principle of redox catalysis relies on the use of an easily reducible redox mediator M associated to an intrinsically stable anion radical $M^{\bullet-}$. By definition, in the organic field this necessitates that M is a very delocalized aromatic molecule the anion radical of which is therefore prone to react with electrogenerated radicals with a rate constant k_{25}:

$$M^{\cdot-} + R^{\cdot} \rightarrow M\text{-}R^{-} \ (+ E^{+} \rightarrow E\text{-}M\text{-}R) \quad (25)$$

where E^+ is an electrophile present in the medium or a metallic cation resulting from the sacrificial anode dissolution.

This process competes with the favorable reduction of $R^{\bullet}$ [Eq. (17)] the rate constant of which is k_{17}, and the competition parameter $q = k_{17}/(k_{17}+k_{25})$ that regulates their competition is independent of the experimental conditions (of the concentration [M] and [RX] of the mediator M and of the substrate RX) since both reactions have the same molecularities. The occurrence of this side reaction [Eq. (25)] has been recognized since the earliest works on redox catalysis[22,23] and more recently it has been used profitably to determine the reduction potential of a wide series of organic radicals.[24] Indeed, the full occurrence of the process shown in Equation (25) corresponds to the complete depletion of M and to the quantitative formation of E-M-R by a two-electron route compared with M, while full occurrence of the reduction portrayed in Equation (17), followed by the coupling of R^- with the electrophile E^+, corresponds to total conservation of M and to the formation of R-E by a two-electron route compared with RX, that is, formally a $1+2([RX]/[M])$-electron route compared with M. Thus, the determination of the relative yields in E-M-R, M, and R-E at the end of an electrolysis, or of the charge consumed, or of the current used in analytical electrochemistry are direct measurements of the competition parameter q. As we just summarized, the ubiquitous occurrence of the radical–radical coupling shown in Equation (25) has been widely used for kinetic purposes, and yet to our knowledge, its consequences on a preparative scale have not been examined from a theoretical point of view.

The second feature that is intrinsic to all redox catalysis processes is that the redox mediator, being a catalyst, undergoes a large number of redox cycles to allow the conversion of the substrate. For example, for the electrocarboxyation that is our main interest in this study, a minimum number $N_{min} = 2([RX]/[M]) \gg 1$ of catalytic cycles is required in order to convert all the RX substrate, even upon assuming an exceptional situation of a 100% Faradaic yield for the electrocarboxylation. Thus, even if the anion radical $M^{\bullet-}$ is sufficiently stable to give rise to a fully chemically reversible voltammetric reduction for M, its stability may not be sufficient to stand unaltered during a long period of electrolysis. Indeed, any slow first-order:

$$M^{\cdot-} \rightarrow \text{etc.} \quad (26)$$

or second-order

$$2\,M^{\cdot-} \rightarrow \text{etc.} \quad (27)$$

decomposition reaction not noticeable at the voltammetric level owing to a rate constant k_{26} or k_{27} too small to be determined, may prove disastrous in industrial applications.

In fact, as mentioned above, if a sufficiently fast charge transfer is involved (high values of k_{ET}),[21] in the portion of the diffusion layer between the electrode surface and the reaction layer no carboxylation reaction occurs and $M^{\bullet-}$ is involved only in the reactions shown in Equations (26) and (27), thus leading to the destruction of a small but non-zero fraction of the redox mediator at each cycle.

These simple considerations show that the "natural" existence of reactions shown in Equations (25) and (26), or (27), in any redox catalytic process amounts to a nearly identical effect since all of them impose a small loss of the redox mediator at each catalytic cycle (rotation). Even if these losses are minimal within each cycle for any process worth to be considered after a voltammetric study, their cumulative effects over the large number of cycle rotations required under preparative conditions may not be negligible at all and may eventually exclude any large scale electrosynthesis application. We wish thus to examine in more detail these preparative consequences for each reaction, before examining the effect of other important side reactions since these are merely related to the reactivity of $R^{\bullet}$ and R^-.

Effect of the coupling between R$^{\bullet}$ and M^{-}: Whenever R$^{\bullet}$ is easily reducible, q is large so that this reaction may be considered initially as a minor side pathway. Yet, M is present at a concentration [M] that is by definition much lower than the concentration of RX. Thus, even if $q = k_{17}/(k_{17}+k_{25})$ is close to unity, the accumulated number of passages at the branching point between the reactions shown in Equations (17) and (25) in each cycle makes the catalyst concentration decrease significantly while the electrocatalysis proceeds. In the following we wish to restrict to a very crude and simplified analysis of the problem as this competition is not among the limiting competitions in our case (see below). Moreover, this simplified analysis illustrates perfectly the problem at hand.

After completion of the jth cycle, the remaining mediator concentration is $([M])_j = ([M])_0 q^j$. Let N be the total number of cycles required for the total conversion of RX. During completion of the jth cycle the RX concentration drops by an amount equal to $([M])_j/2$. The end of the process corresponds to a complete removal of RX, so that $([RX])_N = 0$. This affords the value of N that must then be such as $([RX])_0 \approx ([M])_0/2(1-q^N)/(1-q)$. It then follows that a number $N \approx \log[1-2([RX])_0/([M])_0(1-q)]/\log q$ cycles is required to complete the electrocarboxylation. Note that $N = N_{min} = 2([RX])_0/([M])_0$ when $q = 1$, while RX never reaches total conversion when $q \ll 1$. However, it is important to note also that at the end of the Nth cycle, the redox mediator is $([M])_N = ([M])_0 q^N = ([M])_0 - 2(1-q)([RX])_0$. If we wish that the completion of the electrolysis is performed at a significant rate, $([M])_N$ must remain comparable to $([M])_0$. Let us consider for example that $([M])_N = \alpha([M])_0$ is a minimum operational value, so that one must have $q \geq 1-(1-\alpha)([M])_0/(2([RX])_0)$. If for example the initial concentration of the mediator is 5% of that of RX, and $\alpha = {}^1/_2$, this shows that q must be larger than approximately 0.99, that is, that k_{17} must be at least 80 times larger than k_{25}. This may be difficult to achieve since the radical–radical coupling shown in Equation (25) is expected to be almost activationless.

Despite its crudeness, this simple analysis illustrates perfectly the intrinsic difficulty of performing redox catalysis on an industrial production scale, even when the process is perfectly suited to smaller scales such as in electroanalytical measurements or laboratory-scale electrolysis.

Effect of a first- or second-order slow deactivation of M$^{\bullet-}$: Since we will establish in the following that this competition is among the central ones in our experimental system we wish to present a more complete treatment than that above. Here we do not wish to present a full account of the kinetic competition but only to examine how the system departs from an interesting situation from the electrosynthetic point of view. In particular, with regard to the kinetic structuring of the diffusion layer, as mentioned already, conservation of fluxes around $x = \mu$ (where x is the distance from the cathode surface and μ is the distance from the reaction layer to the electrode surface) imposes that:

$$-0.5\left(\frac{d[M^{\bullet-}]}{dx}\right)_{\mu^-} = \left(\frac{d[RX]}{dx}\right)_{\mu^+} = \frac{[RX]^{bulk}}{(\delta-\mu)} \quad (28)$$

when we assume an identical diffusion coefficient D for all species (note that reduction of one RX molecule involves the consumption of two M$^{\bullet-}$ anion radicals).

Within the thin kinetic layer ($0 < x < \mu$), M$^{\bullet-}$ anion radicals diffuse and react exclusively through the slow reactions shown in Equations (26) and (27), so that:

$$\frac{d^2[M^{\bullet-}]}{dx^2} = \frac{k_{26}[M^{\bullet-}] + k_{27}[M^{\bullet-}]^2}{D} \quad (29)$$

Multiplication of both sides of Equation (29) by $(d[M^{\bullet-}]/dx)$ and integration over x from $x = 0$ to $x = \mu$, yields:

$$\left[\left(\frac{d[M^{\bullet-}]}{dx}\right)_0\right]^2 = \left[\left(\frac{d[M^{\bullet-}]}{dx}\right)^{\mu-}\right]^2 + \{k_{26} + {}^2/_3 k_{27}[M^{\bullet-}]_0\}[M^{\bullet-}]_0^2/D \quad (30)$$

$(d[M^{\bullet-}]/dx)_0$ corresponds to the overall current i that flows through the cell (note that we thus implicitly assume the simplification that the two decomposition reactions correspond to one-electron processes), so that $\{(d[M^{\bullet-}]/dx)_0\}^2 = (i/FAD)^2$ (F = Faraday constant, A = surface area of the electrode). Combination of Equations (28) and (30) thus affords:

$$\left(\frac{i}{FAD}\right)^2 = \left(\frac{2[RX]^{bulk}}{\delta-\mu}\right)^2 + \left(\frac{k_{26} + {}^2/_3 k_{27}[M^{\bullet-}]_0\}[M^{\bullet-}]_0^2}{D}\right) \quad (31)$$

thus reflecting the instant Faradaic efficiency of the system since i is the overall electrolysis current, while $2FAD[RX]^{bulk}/(\delta-\mu)$ is that used for the effective two-electron reduction of RX. Thus, the Faradaic yield y_F is defined by $2FAD[RX]^{bulk}/i(\delta-\mu)$ and is given by:

$$y_F = \frac{1}{\left[1 + \{k_{26} + {}^2/_3 k_{27}[M^{\bullet-}]_0\}\left(\frac{(\delta-\mu)^2}{4D}\right)\left(\frac{[M^{\bullet-}]_0}{[RX]^{bulk}}\right)^2\right]^{1/2}} \quad (32)$$

The expression in Equation (32) shows how the existence of these spontaneous decomposition reactions affect the Faradaic yield, yet as noted above this does not affect the chemical yield of the electrocarboxylation. Here, we wish to examine how these reactions force the system to depart from an ideal behavior. Thus, provided the reaction may proceed to completion, Equation (32) can be simplified by considering that in a catalytic process $[M^{\bullet-}]_0$ is significantly lower than $[RX]^{bulk}$ and as a consequence $\{(\delta-\mu)/\delta\}$ approaches unity [see Eqs. (23) and (24)]. Thus, Equation (32) simplifies to:

$$y_F \approx \frac{1}{\left[1+\lambda\{([M^{\cdot-}]_0/[RX]^{bulk})^2\}\right]^{1/2}} \quad (33)$$

where $\lambda=\lambda_1+2\lambda_2/3$, λ_1 and λ_2 being defined by:

$$\lambda_1 = k_{26}\left(\frac{\delta^2}{4D}\right) \quad (34)$$

$$\lambda_2 = k_{27}\left([M^{\cdot-}]_0\frac{\delta^2}{4D}\right) \quad (35)$$

$\lambda=\{k_{26}+{}^2/_3k_{27}([M^{\bullet-}]_0\}(\delta^2/4D))$ is therefore the dimensionless kinetic parameter controlling the effect of reactions given in Equations (26) and (27) under our conditions.

To proceed, we need to evaluate the values of $[M^{\bullet-}]_0$ of the concentration of the anion radical $M^{\bullet-}$ at the electrode surface. For that, since we examine only the departure from an ideal situation, we consider that $k_{26}\mu^2/D$ and $k_{27}[M^{\bullet-}]_0\mu^2/D$ are sufficiently small to have only a minor effect on the conservation of the mediator mass at each moment of electrolysis. This implies that the profile of the anion radical $M^{\bullet-}$ is almost linear. Hence, at any distance x from the electrode surface:

$$[M]^{bulk} = [M^{\cdot-}]_x + [M]_x \quad (36)$$

Since the $M/M^{\bullet-}$ redox couple is Nernstian by definition, we obtain:

$$[M^{\cdot-}]_0 = [M]^* \quad (37)$$

where $[M]^*$ is given by Equation (24).

The combination of Equations (23), (33), and (37) finally affords the expression of y_F within our approximation level:

$$y_F \approx \frac{1}{\left[1+\lambda([M]^*/[RX]^{bulk})^2\right]^{1/2}} \approx \frac{1}{\left[1+(\lambda_1+2\lambda_2/3)([M]^*/[RX]^{bulk})^2\right]^{1/2}} \quad (38)$$

where $[M]^*$, λ_1, and λ_2 are defined in Equations (24), (34), and (35), respectively.

When expressed as $\Delta[M]^{bulk}/\Delta[RX]^{bulk} = ([M]^0-[M]^{bulk})/([RX]^0-[RX]^{bulk})$, the average decomposition of the redox mediator per rotation is given by $(1-y_F)/y_F$. Thus, one obtains by using the expression of y_F in Equation (38):

$$\left[\frac{\Delta[M]^{bulk}}{\Delta[RX]^{bulk}}+1\right]^2 = 1+\lambda\left(\frac{[M]^*}{[RX]^{bulk}}\right)^2 \quad (39)$$

Since the redox mediator concentration is by definition significantly lower than that of the substrate and λ is small since we examine only departure from an ideal process, Equation (39) simplifies into:

$$\frac{\Delta[M]^{bulk}}{\Delta[RX]^{bulk}} \approx \left(\frac{[M]^*}{[RX]^{bulk}}\right)^2\lambda/2 \quad (40)$$

Equation (40) establishes that in any given situation (namely, given λ_1 and λ_2) the $\Delta[M]^{bulk}/\Delta[RX]^{bulk}$ ratio varies rapidly with the excess factor $\gamma^*=[RX]^{bulk}/[M]^*$. This is particularly important since it is desirable that the $[RX]^{bulk}$ decreases faster than $[M]^*$ to maintain a sufficient rate of electrolysis while the electrocarboxylation proceeds to completion.

In particular, during the synthesis both $[M]^*$ and $[RX]^{bulk}$ and their ratio varies during the electrolysis. Thus, Equation (40) should be written in differential terms as

$$\frac{d[M]^{bulk}}{d[RX]^{bulk}} \approx \left(\frac{[M]^*}{[RX]^{bulk}}\right)^2\lambda/2 \quad (41)$$

that by integration, gives rise to:

$$\frac{[M]^0}{[M]}-1 \approx [M]^0(\sigma/2)\left(\frac{1}{[RX]}-\frac{1}{[RX]^0}\right) \quad (42)$$

where now all concentrations refer only to the bulk solution, so that the superscript "bulk" is no longer indicated and $\sigma=\lambda/\{1+\exp[F(E-E^0_M)/RT]\}^2$. Remarking that in our first-order level of approximation, essentially all the charge passed (Q) serves to reduce RX, one has $[RX]^{bulk}\approx[RX]^0-Q/2FV$ where $[RX]^0$ is the initial concentration of RX in the bulk solution of volume V (note that this is true irrespective of the potentiostatic or galvanostatic conditions), one obtains:

$$\frac{[M]}{[M]^0} \approx \frac{1}{\left\{1+\frac{\sigma}{2}\frac{[M]^0}{[RX]^0}\frac{Q}{Q^{th}-Q}\right\}} \quad (43)$$

where $Q^{th}=2F[RX]^0\cdot V$ is the theoretical charge required to complete a would-be 100% efficient electrolysis, that is, when no catalyst deactivation occurs (namely, when $\lambda=0$).

This means therefore that the existence of intrinsic redox mediator deactivation routes [Eqs. (26) and (27)] causes the amount of catalyst to decrease with the RX conversion even when these reactions are sufficiently slow to be almost unnoticeable by means of cyclic voltammetry. This is a particularly important result since it is almost impossible for any radical anion to be perfectly stable. Since the deactivation corresponds to a loss of the mediator, one may be tempted to counterbalance this loss by using a larger initial concentration of mediator or by reintroducing it in the cell while the electrolysis proceeds. Equation (38) shows that this intuitive method is actually counterproductive with respect to the yield. In fact, from this equation we deduce that to

maintain the yield close to unity, one must maintain $[RX]^0/[M]^*$ as large as possible by either decreasing the cathode potential (namely, making it less negative) so that $[M]^*$ decreases or by adding RX to the bulk solution. The experimental validity of these counter-intuitive actions will be demonstrated in the following experimental investigation.

Effect of side reactions involving $R^\cdot$ or R^-: The two above analyses are almost independent of the exact nature of the redox catalytic process under investigation because they are fundamentally rooted in the very principle of redox catalysis itself and not in the catalyzed reaction. Instead, competitive reactions involving the transient reactive intermediates $R^\cdot$ (except for that related to Equation (25) that consumes the redox mediator and the effect of which has already been examined) and R^- do not affect the redox catalytic process but only the selectivity of the sought catalyzed process, since the presence of such competitive pathways amounts only to a change in the destination of the charge that continues to be delivered by the redox mediator. Thus, the two series of competitive pathways (namely, those involving $M^{\cdot-}$, and those involving only $R^\cdot$ and R^-) have different fundamental effects on the process. This is the reason why we separated the two classes of reactions.

As deduced from the above analysis of the structuring of the diffusion layer during an efficient redox catalysis, and in contradiction with the usual situation observed in direct electrolysis, $R^\cdot$ and R^- exist only in the thin reaction layer located in the diffusion layer around $x=\mu$. Here they are maintained at trace levels because there is a steady state established between their production and consumption rates. This explains why bimolecular reactions involving these species are seldom observed in redox catalysis. For example, one observes generally no dimerization (namely, formation of R_2) nor dismutation (namely, equimolar formation of R(−H) and R−H) of radicals $R^\cdot$ even when the same species easily undergoes these exergonic pathways under other chemical circumstances. However, this is obviously not true for first-order reactions involving these reactive species since their local concentration is then kinetically irrelevant. Let then:

$$R^\cdot \rightarrow \text{and so on} \tag{44}$$

and

$$R^- \rightarrow \text{and so on} \tag{45}$$

are the prototypes of each series of competitive reactions with respective overall pseudo-first-order rate constants k_{44} and k_{45}. The reaction shown in Equation (44) (most usually a hydrogen atom transfer reaction) is then in competition with the radical reduction by $M^{\cdot-}$ [Eq. (17)], while the reaction shown in Equation (45) (usually a protonation) competes with the nucleophilic addition of R^- onto CO_2 (the reaction shown in Equation (4), the rate constant of which is k_4). Again we are interested only in situations where the mediated electrocarboxylation is efficient and we wish only to examine here how the occurrence of such competitive processes make it depart from a 100% yield. Thus we voluntarily create the situation where these competitions are first-order perturbations so that they can be treated as being independent between themselves or from the two above competitive routes involving $M^{\cdot-}$. In such a first-order approximation, the overall electrolysis yield Y is given by the product of the two individual yields since the two branching points are consecutive in the overall mechanism. Thus:

$$Y = y(R^\cdot)y(R^-) \tag{46}$$

where $y(S)$ is the individual yield of the competition involving the species S.

$R^\cdot$ is under chemical steady state between its production by the reactions shown by Equations (15) or (16) (rate: $k_{ET}[M^{\cdot-}][RX]$) and its consumption by the sum of the reactions shown in Equations (17) and (44) (overall rate: $(k_{17}[M^{\cdot-}]+k_{44})[R^\cdot]$). Thus, $[R^\cdot] = k_{ET}[M^{\cdot-}][RX]/(k_{17}[M^{\cdot-}]+k_{44})$. This concentration differs from zero only within a thin strip of solution of thickness Δ centered on $x=\mu$, since the product $[M^{\cdot-}][RX]$ differs from zero only within this very thin domain. Within this domain, $[RX]\approx(x-\mu+\Delta/2)[RX]^{bulk}/(\delta-\mu+\Delta/2)$ and $[M^{\cdot-}]\approx(\mu+\Delta/2-x)2[RX]^{bulk}/(\delta-\mu+\Delta/2)$ by extrapolating the linear concentration profiles of each species outside this zone. Also, since we examine only how the system departs from the ideal behavior, the concentration of $R^\cdot$ within this thin strip may be approximated by $[R^\cdot] = (k_{ET}/k_{17})[RX]$ by neglecting the effect of the reaction given in Equation (44) at this stage. On the other hand, at any moment of electrolysis, the instant yield $y(R^\cdot)$ is given by the ratio of integrals corresponding to each reaction over the domain of thickness Δ:

$$y(R^\cdot) = \frac{k_{17}\int_{\mu-\Delta/2}^{\mu+\Delta/2}[R^\cdot][M^{\cdot-}]dx}{k_{17}\int_{\mu-\Delta/2}^{\mu+\Delta/2}[R^\cdot][M^{\cdot-}]dx + k_{44}\int_{\mu-\Delta/2}^{\mu+\Delta/2}[R^\cdot]dx} \tag{47}$$

Evaluation of the two integrals in Equation (47) based on the above approximation and substitution of μ by Equation (23) gives:

$$y(R^\cdot) \approx \frac{1}{1+3(\frac{\delta}{\Delta})k_{44}/[k_{17}(2[RX]^{bulk}+[M]^{bulk})]} \tag{48}$$

that, for sufficiently high value of the ratio $[RX]^{bulk}/[M]^{bulk}$ gives:

$$y(R^\cdot) \approx \frac{1}{1+\left(\frac{3\delta}{2\Delta}\right)\left(\frac{k_{44}}{k_{17}[RX]^{bulk}}\right)} \tag{49}$$

This result shows that because of the presence of the term δ/Δ that is by definition considerably larger than unity, the

reduction of R$^{\bullet}$ is disfavored as soon as k_{44}/k_{17} is not negligible. This confirms a well-known experimental result since it has been established previously that redox catalysis is a very convenient way for favoring the reaction of radicals produced by electroreduction of organic halides through pseudo-first-order non-reductive pathways (for example, reactions with nucleophiles in $S_{RN}1$-like reactions, rearrangements, addition to unsaturated systems, atom abstraction, and so forth). Here we would like the opposite (namely, a quantitative reduction of R$^{\bullet}$) and the electrolytic medium must be chosen to minimize reactions such as those portrayed in Equation (44) occur. In this respect it is worth mentioning that an indirect consequence of using sacrificial anodes and a single-compartment cell is beneficial since this allows the introduction of low concentrations of the tetraalkylammonium supporting electrolyte. Indeed, lowering the concentration of these efficient hydrogen atom donors decreases the magnitude of k_{44} and favors the reduction of the radical.

The evaluation of $y(R^-)$ is more straightforward since it involves a competition between reactions of identical molecularities. Thus, it depends only on the ratio of pseudo-first-order constants:

$$y(R^-) \approx \frac{1}{1+\frac{k_{45}}{k_4[CO_2]}} \tag{50}$$

The problem is, however, more delicate when the RX substrate itself is the proton donor involved in the reaction portrayed by Equation (45) (father–son mechanism, see below):

$$R^- + RX \rightarrow RH + {}^-R(\text{-H})X\ (\rightarrow R(\text{-H}) + X^-) \tag{51}$$

Then the rate of the reaction in Equation (45) is expressed as $k_{51}[RX][R^-]$, where R^- is under chemical steady state between its production by the reaction in Equation (17) (rate $k_{17}[R^{\bullet}][M^{\bullet -}] \approx k_{ET}[RX][M^{\bullet -}]$, see above) and its consumption by reactions shown in Equation (4) and (51) (overall rate: $(k_{51}[RX]+k_4[CO_2])[R^-]$) so that within the thin strip of solution of thickness Δ centered on $x=\mu$ one has $[R^-] \approx k_{ET}[RX][M^{\bullet -}]/(k_{51}[RX]+k_4[CO_2])$, and $[R^-] \approx 0$ outside this domain. Again we consider only minor deviations from the ideal mediated electrocarboxylation so that $[R^-] \approx k_{ET}[RX][M^{\bullet -}]/(k_4[CO_2])$ and we may approximate the concentrations of RX and $M^{\bullet -}$ by the above expressions within the thin domain of thickness Δ. Thus, $y(R^-)$ that is expressed as:

$$y(R^-) = \frac{k_4 \int_{\mu-\Delta/2}^{\mu+\Delta/2} [R^-][CO_2]dx}{k_4 \int_{\mu-\Delta/2}^{\mu+\Delta/2} [R^-][CO_2]dx + k_{51} \int_{\mu-\Delta/2}^{\mu+\Delta/2} [R^-][RX]dx} \tag{52}$$

simplifies into:

$$y(R^-) = \frac{\int_{\mu-\Delta/2}^{\mu+\Delta/2} [RX][M^{\bullet -}]dx}{\int_{\mu-\Delta/2}^{\mu+\Delta/2} [RX][M^{\bullet -}]dx + \frac{k_{51}}{k_4[CO_2]} \int_{\mu-\Delta/2}^{\mu+\Delta/2} [M^{\bullet -}][RX]^2 dx} \tag{53}$$

that then gives:

$$y(R^-) \approx \frac{1}{\{1+(\Delta/2(\delta-\mu))(k_{51}[RX]^{bulk})/(k_4[CO_2])\}} \approx \frac{1}{1+\left(\frac{\Delta}{2\delta}\right)\frac{k_{51}[RX]^{bulk}}{k_4[CO_2]}} \tag{54}$$

Equation (54) shows that the fact that the reaction between R^- and RX may occur only within the thin strip around $x=\mu$ disfavors the reaction shown in Equation (51), because the ratio $k_{51}[RX]^{bulk}/k_4[CO_2]$ is then multiplied by the very small term $\Delta/2\delta$. This is the opposite conclusion to the previous case concerning the side reaction of R$^{\bullet}$. Indeed, Equation (54) shows that a mediated process is more advantageous than a direct electrocarboxylation, because the effect of the side reaction shown in Equation (51) is spontaneously diminished.

The examination of the two above competitions establishes that the value Δ/δ plays a crucial role in disfavoring the occurrence of bimolecular reactions involving the transient intermediates R$^{\bullet}$ or R^- with their kinetic parent species $M^{\bullet -}$ or RX because these later species are maintained at extremely small values within the thin strip of thickness Δ, where only R$^{\bullet}$ and R^- can exist. The thickness of this strip has been previously estimated[21] as $\Delta/\delta \approx 7.4\ (\mu/\delta)(k_{ET}[M]^{bulk}\mu^2/D)^{-1/3} \approx 6/(k_{ET}[RX]^{bulk}\delta^2/D)^{1/3}$ when more than 99% of the $RX^{\bullet -}$ and M regeneration occurs within this domain of solution.

Experimental discussion

Experimental investigations in preparative-scale electrolysis: The above theoretical analysis has allowed to delineate several built-in factors that make the use of redox catalysis difficult on the preparative scale in a general situation and that are, in our view, the very reason why this technique has not yet found many industrial applications despite the other numerous advantages it offers. However, identifying these intrinsic difficulties simultaneously offers the way to counterbalance their negative effects. In the following we wish to illustrate how this can be performed successfully with the electrocarboxylation of 1-phenyl-1-chloroethane.

This substrate was chosen as a prototype of the benzylic halides; the carboxylation of which at the α carbon leads to a wide variety of anti-inflammatory drugs, but also because it is a particularly suited example to test our above conclusions. Firstly, it bears a benzylic chlorine that is less likely to undergo a direct electrocarboxylation or an organometallic-

catalyzed electrosynthesis than the bromine or iodine analogues. Secondly, the fact that the halogen-bearing benzene substituent is an ethyl chain making it suitable to undergo an elimination-type reaction [compare reaction shown in Equation (51)]:

$$\mathrm{Ph{-}C^{-}(H){-}CH_3 + Ph{-}CHCl{-}CH_3 \rightarrow Ph{-}CH_2{-}CH_3 + Ph{-}C(H){=}CH_2 + Cl^{-}} \quad (55)$$

Hence, our above conclusions can be tested.

Conversely, the intrinsic stability of the benzyl radical hinders its coupling with the reduced form of the redox mediator (so that a wide series of mediators can be compared without introducing any bias in the experiments) or any hydrogen-atom abstraction from the supporting electrolyte/solvent system (nBu$_4$NBr/dimethylformamide or 1-methyl-2-pyrrolidone). Indeed a previous study,[7] confirmed by the present investigation (see below), has shown that, under particular operative conditions and in the presence of aromatic esters as mediators, very low consumption of mediator, corresponding to a value of q larger than approximately 0.99, is observed as a possible result of both the intrinsic stability of the benzyl radical and the steric hindrance of the couple mediator–benzyl radical. Thus conductive conditions could be used to allow a proper control of the working electrode potential since we have shown this to be crucial through its effect on the value of [M]*. For the same reason, the preparative experiments have been performed under potentiostatic conditions although galvanostatic conditions are generally preferred in industrial applications.

This system was previously investigated by some of us so that a documented experimental investigation of its behavior already existed before this work was initiated.[7] In particular, it has thus been shown that irrespective of the cathode material a progressive electrode blocking occurs during direct electroreductions so that large-scale electrolyses could not be performed to completion. This disadvantageous phenomena was suppressed when the process was conducted through redox catalysis. In this former study an extended series of catalysts was examined, and adequate conditions could then be found to perform a successful mediated electrocarboxylation at the scale of a few grams with minimal production of side products. However, the potentially most adequate mediators with respect to the competitive oxalate production, that is, those with the more positive reduction potential (see above), have been observed to undergo a drastic consumption during the electrolyses so that electrocarboxylations could be performed up to completion only with difficulty. This deactivation stems from the intrinsic stability of the anion radical of the mediators since no coupling product with the 1-phenylethane radical was observed. This effect was the most apparent for 1,3-benzenedicarboxylic acid dimethyl ester so that this mediator was selected to conduct the present study. This indeed allowed precise measurements of the various factors that affect the deactivation rate.

General overview of the system: Putting aside the above-mentioned catalyst consumption, electrolysis of 1-phenyl-1-chloroethane mediated by 1,3-benzenedicarboxylic acid dimethyl ester in permanently saturated carbon dioxide solutions affords the expected benzylic carboxylate together with oxalate and minor amounts of styrene and phenylethane. Importantly, the yield of oxalate decreases upon increasing the value of $[RX]^{bulk}/[CO_2]$, while that of styrene increases with the same factor, so that the yield of the required carboxylate presents a maximum with this parameter (Figure 2). This establishes several points.

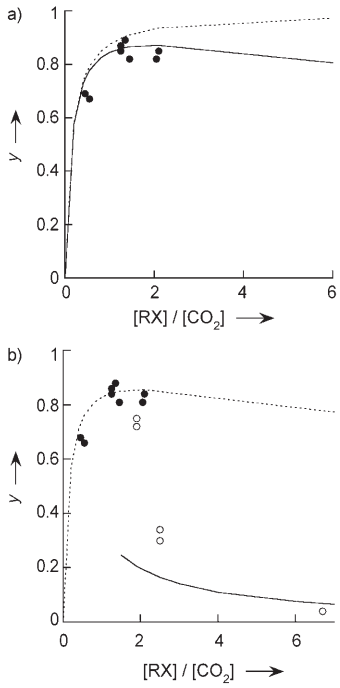

Figure 2. a) Influence of the $[RX]/[CO_2]$ ratio on the yield of carboxylate: experimental data (●), fitted data by the expression in Equation (59) with $\varepsilon_H=0$ (——) and $\varepsilon_H=\zeta=0$ (-----). [RX] from 0.06 to 0.3 M; SSE: NMP 0.1 M Bu_4NBr; CO_2 saturated, atm pressure ($[CO_2]=0.14$ M); $E=E^0-0.17$ V. b) Influence of the $[RX]/[CO_2]$ ratio on the yield in carboxylate: Experimental data obtained with constant concentration of carbon dioxide 0.14 M (●) and substrate 0.2 M (○), fitted data by the expression in Equation (59) (-----) and Equation (62) (——). [RX] from 0.06 to 0.3 M; $[CO_2]$ from 0.03 to 0.14 M; SSE: NMP 0.1 M Bu_4NBr; $E=E^0-0.17$ V.

Firstly, the fact that styrene production increases upon increasing $[RX]^{bulk}/[CO_2]$ while keeping $[RX]^{bulk}$ constant rules out its formation through the dismutation of benzyl radicals, since carbon dioxide would not be involved in this competition.

$$\mathrm{2\,Ph{-}C^{\cdot}(H){-}CH_3 \rightarrow Ph{-}CH_2{-}CH_3 + Ph{-}C(H){=}CH_2} \quad (56)$$

This supports our previous statement that the concentration of R$^{\bullet}$ is too small under redox catalytic conditions to allow

any bimolecular reactions between these radicals. Conversely, the observed behavior is perfectly compatible with the occurrence of a reaction between the benzylic anion and its parent RX [Eq. (55)]. Indeed, Equation (54) predicts that whenever a competition between such a reaction and the carboxylation of the anion occurs, the yield in styrene must increase upon increasing $[RX]^{bulk}/[CO_2]$ either by increasing the $[RX]^{bulk}$ or decreasing the $[CO_2]$.

Within this simple framework, styrene and phenylethane should be produced in equimolar amounts and the yield of phenylethane should not depend on the presence of an added proton donor. However, slightly more phenylethane than styrene is produced (data not shown) and the phenylethane production increases upon addition of water as a proton donor in the cell. Thus we need to consider also that in the absence of added water a small fraction of the phenylethane observed is formed by protonation of the benzylic anion as stated before, (note that a hydrogen atom transfer to the benzyl radical would yield also to phenylethane; yet we may discard this route owing to the large stabilization of the secondary benzylic radical). Under these conditions, Equation (54) must then be slightly amended to account for the effect of the protonation of R^- by the medium, so that (compare Eq. (50)]:

$$y(R^-) \approx \frac{1}{\frac{1+\{k_H[DH]+(\frac{\Delta}{2\delta})k_{51}[RX]^{bulk}\}}{k_4[CO_2]}} \quad (57)$$

where k_H is the rate constant of the protonation by the medium and DH the proton donor [compare Eq. (45)].

Secondly, the fact that the oxalate yield decreases upon increasing the concentration ratio $[RX]^{bulk}/[CO_2]$ indicates that the mediator anion radical may competitively reduce the benzyl chloride substrate and the carbon dioxide. We have not examined this competition in our theoretical investigation but based on the above analyses we note that the yield of $R^{\bullet}$ for electrocarboxylation is then given by:

$$y^* \approx \frac{1}{\left(1+\left(\frac{3\delta}{\Delta}\right)\left(\frac{k_{21}[CO_2]^{bulk}}{k_{ET}[RX]^{bulk}}\right)\right)} \quad (58)$$

where k_{21} is the rate constant of the homogeneous reduction of CO_2 by $M^{\bullet -}$ [Eq. (21)] that leads to the carbon dioxide anion radicals that afford oxalate by fast dimerization [Eq. (22)].

The overall carboxylate yield is approximated by the product of the partial yields in Equations (57) and (58). Denoting ρ to be the rate ratio $([RX]^{bulk})/[CO_2]$ $(k_{ET}/k_{21})(\Delta/3\delta)$, one obtains:

$$y(\rho) = \frac{\rho}{[(1+\rho)(1+\varepsilon_H+\zeta\rho)]} \quad (59)$$

where $\zeta = {}^3/_2[(k_{51}/k_4)(k_{21}/k_{ET})]$, and $\varepsilon_H = (k_H/k_4)([DH]/[CO_2])$. This expression predicts that the yield of carboxylate is a bell-shaped function of $[RX]^{bulk}/[CO_2]$, presenting a maximum $[y(\rho)]_{max} = 1/[\zeta^{1/2}+(1+\varepsilon_H)^{1/2}]^2$ for $\rho_{max}=[(1+\varepsilon_H)/\zeta]^{1/2}$, and such as $y(\rho)\propto\rho/(1+\varepsilon_H)\rightarrow 0$ when $\rho\rightarrow 0$ or $y(\rho)\propto 1/\zeta\rho$ when $\rho\rightarrow\infty$. This compares satisfactorily with the results presented in Figure 2a. The best fit of these results by the expression in Equation (59) indicates that ε_H is at maximum equal to 0.02, in agreement with the small excess of phenylethane production versus that of styrene. On the other hand, the experimental data show that the maximum of the carboxylate yield is broad, so that it does not depend drastically on $[RX]^{bulk}/[CO_2]$ after its maximum. This reflects that k_{51}/k_4 is small so that the parameter ζ is also small. In other words, in our experimental window, the system does not depend much on the corresponding competition except at very small but unrealistic values of $[RX]^{bulk}/[CO_2]$. Note that it would nevertheless influence the yield at considerably large $[RX]^{bulk}/[CO_2]$ values as evidenced by the comparison of the two plots in Figure 2a.

To probe the system behavior at larger $[RX]^{bulk}/[CO_2]$ values, we decided to decrease the carbon dioxide bulk concentration while keeping $[RX]^{bulk}$ at 0.2 M. The corresponding data are shown in Figure 2b with open symbols. However, it is clear from the results that the yield no longer follows the prediction given in Equation (59), the decay at large $[RX]^{bulk}/[CO_2]$ values being too steep. We thus presume that this behavior reflects another phenomenon that occurs when $[CO_2]$ is too low. Indeed, in the above derivations we implicitly assumed that the carbon dioxide bulk concentration, its rate of dissolution, and its diffusion coefficient D_{CO_2}, relative to that D_{RX} of RX, were all high enough to maintain the carbon dioxide concentration at $[CO_2]^{bulk}$, imposed by its dissolution equilibrium, even in the thin strip around $x=\mu$ where it reacts with R^-. However, when the concentration of CO_2 becomes too small compared with that of RX (note that one equivalent of CO_2 is consumed per RX converted into carboxylate) this cannot be true anymore. In the limiting case of a very small concentration of CO_2, it becomes of the order of $(\Delta/2\delta)[CO_2]^{bulk}$ around $x=\mu$, being limited by its diffusion. In this extreme situation Equation (57) becomes:

$$y'(R^-) \approx \frac{1}{1+\{(\frac{2\delta}{\Delta})k_H[DH]+k_{51}[RX]^{bulk}\}/\{k_4[CO_2]^{bulk}\}} \quad (60)$$

The same is true for Equation (58) that needs to be rewritten as:

$$y'^* \approx \frac{1}{1+\left\{\left(\frac{3k_{21}}{2k_{ET}}\right)\frac{[CO_2]^{bulk}}{[RX]^{bulk}}\right.} \quad (61)$$

so that the overall yield in carboxylate, $y' = y'(R^-)y'^*$, becomes:

$$y'(\rho') = \frac{\rho\prime}{[(1+\rho')(1+\varepsilon'_H+\zeta\rho')]} \quad (62)$$

where ρ' is the ratio $(k_{ET}/k_{21})(2[RX]^{bulk})/3[CO_2]$, and $\varepsilon'_H = (2\delta/\Delta)(k_H/k_4)([DH]/[CO_2])$. As expected, this equation has the same overall structure as Equation (59), yet the order of magnitude of the parameters differs drastically so that the variations of y' may be quite different from those of y shown in Figure 2a. This explains why the two series of experimental data (open and filled symbols) shown in Figure 2, do not exhibit the same behavior for comparable values of $[RX]^{bulk}/[CO_2]^{bulk}$, as evidenced for example by the comparison of the two plots shown in Figure 2b (note that Equation (62) is plotted only for $[RX]^{bulk}/[CO_2]^{bulk}$ ratios that exceed unity, since the approximation leading to its derivation has no meaning in the converse situation. Similarly in this domain $\rho' = \rho(2\delta/\Delta) \gg \rho$, because $\delta \gg \Delta$, so that $y'(\rho') \approx (1+\varepsilon'_H+\zeta\rho')$ in this range). We see that the transition between both limiting cases occurs for $[RX]^{bulk}/[CO_2]^{bulk} \approx 1$ as expected for a titration of carbon dioxide in the diffusion layer. We did not theoretically investigate the cumbersome transition because it is meaningless from an operative point of view. Indeed, it amounts to limit the efficiency of the electrocarboxylation by having too small a concentration of carbon dioxide compared with the stoichiometric requirement.

The expression of the yield in Equation (59) agrees satisfactorily with our experimental results in the experimental range of interest (Figure 2a). Furthermore, it shows that the maximum maximorum yield achievable by a variation of $[RX]^{bulk}/[CO_2]$ only is $[y(\rho)]_{max} = 1/(1+\varepsilon_H)$. Since [DH] is a priori fixed at a minimum value in a given medium, optimizing this maximum requires that we perform the electrocarboxylation with the largest carbon dioxide concentration feasible, that is, under permanently saturated CO_2. Then, ε_H has its minimum value $\varepsilon_{sat} = (k_H/k_4)([DH]/[CO_2]_{sat})$, and $\rho = \rho_{sat} = ([RX]^{bulk})/[CO_2]_{sat}(k_{ET}/k_{21})(\Delta/3\delta)$, so that the maximum efficiency (Figure 2) requires that:

$$[RX]_{max} \approx \frac{k_{21}^{1/2}}{k_{ET}^{1/2}}[CO_2]_{sat}(1+\varepsilon_{sat})^{1/2}\left(\frac{\delta}{\Delta}\right)\left(\frac{6k_4}{k_{51}}\right)^{1/2} \quad (63a)$$

Since, as already mentioned, Δ/δ can be roughly estimated by the expression $\Delta/\delta \approx 6/(k_{ET}[RX]^{bulk}\delta^2/D)^{1/3}$, we obtain:

$$[RX]_{max}^{2/3} \approx \frac{k_{21}^{1/2}}{k_{ET}^{1/6}}[CO_2]_{sat}(1+\varepsilon_{sat})^{1/2}\left(\frac{\delta^2}{D}\right)^{1/3}(k_4/6k_{51})^{1/2} \quad (63b)$$

Thus the maximum maximorum is achieved for $[RX]_{max}^{2/3} = \Lambda k_{21}^{1/2}/k_{ET}^{1/6}$ where $\Lambda = [CO_2]_{sat}(1+\varepsilon_{sat})^{1/2}(\delta^2/D)^{1/3}(k_4/6k_{51})^{1/2}$ is a constant value for a given organic halide electrolyzed in a given medium, that is, when the mediator is changed.

From an operative point of view, on the one hand we are interested in performing electrocarboxylation by using the largest feasible bulk concentration of RX since this causes an increase in the electrocarboxylation rate and decreases the cell volume. On the other hand, other considerations such as the minimization of ohmic heating in the cell (the joule power dissipated in the cell is proportional to the square of the current density, that is, to $([RX]^{bulk})^2$) and adjustment of the electrolysis rate, that is proportional to $[RX]^{bulk}$ and to the rate of dissolution of CO_2 in the electrolyte (see above, Figure 2b) may require a smaller RX concentration. Therefore, from the point of view of the cell operation, for a given cell and external set up, there is an optimum RX concentration, denoted as $[RX]_{cell}$. Optimization of the process requires the conciliation of as many of the mechanistic requirements (namely, $[RX]^{bulk} = [RX]_{max}$) and the cell-operation constraints (namely, $[RX]^{bulk} = [RX]_{cell}$) as possible. This is done by selecting the redox mediator so that the equality $k_{21}^{1/2}/k_{ET}^{1/6} = ([RX]_{cell}^{2/3}/\Lambda)^2$ is verified as closely as possible.

We know from the previous study of this system[7] that the rate constant of the forward electron transfer from $M^{\bullet -}$ to RX [Eqs. (15) or (16)] and to CO_2 obey different linear free energy relationship with their driving force, namely, with E_M^0. Therefore, and neglecting for the present any consideration about the mediator stability (see below), the above requirement is fulfilled by selecting a mediator with a standard potential such as:

$$(E_M^0)_{opt} \approx -\{^2/_3\log([RX]^{bulk}) - \log\Lambda + (\frac{\eta_{ET}}{6} - \frac{\eta_{21}}{2})\}/(\frac{\kappa_{21}}{2} - \frac{\kappa_{ET}}{6}) \quad (64)$$

where κ_j and η_j ($j = 21$ or ET) are respectively the slope and intercept of the linear free energy correlation $\partial(\log\kappa_j)$ versus $\partial(-E_M^0)$ observed experimentally for k_{21} and k_{ET} ($\kappa_{21} = 11.4$, $\eta_{21} = -21$, $\kappa_{ET} = 3.64$ 5, $\eta_{ET} = -3.68$ for the very similar compound 1-(4-isobutylphenyl)-1-chloroethane).[7,20] Therefore, even if the level of approximation used in developing our analyses is too low to be appropriate for an accurate determination of $(E_M^0)_{opt}$, the analyses provide good guidelines for the qualitative description of the system. In particular, by estimating ε_{sat} and k_4/k_{51} by experimental data fitted by using Equation (59), we can roughly estimate $(-E_M^0)_{opt} \approx 1.97$–$2.07$ V with an $[RX]^{bulk} \approx 0.1$ M. Indeed, in a previous study,[7] it has been shown that the Faradaic yields in the target acid depend on the standard redox potential of the catalyst and show maximum values when mediators with an E^0 values between -1.9 and 2.0 V are used.

The above theoretical results are in total agreement with all the empirical observations performed during the previous experimental investigation as well as with all experimental results presented in this work. Therefore, these previous experimental findings are rationalized and the previous assumption that the mediated electrocarboxylation proceeds as summarized in Scheme 1 is validated. However, we left aside the important question of the redox mediator stability during a large-scale electrolysis duration in this analysis. For example, the relationship in Equation (64) assumes that $M^{\bullet -}$ is perfectly stable so that only its thermodynamic (E_M^0) and kinetic (κ and η) redox properties matter. We now wish to

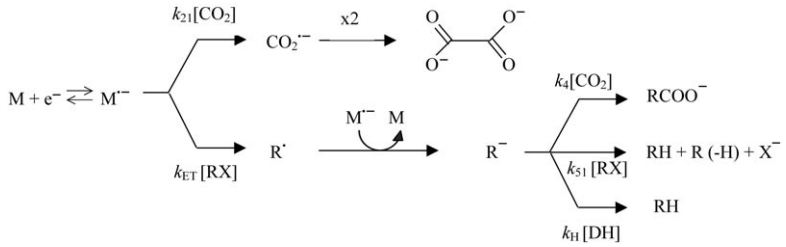

Scheme 1.

consider the influential aspects related to the possible existence of side reactions leading to the mediator consumption.

Deactivation of redox catalysis due to mediator consumption during electrolyses: As explained above, the 1,3-benzenedicarboxylic acid dimethyl ester redox mediator is selected here to test the validity of our model. Indeed, it was found to be among the optimum catalysts based on its reduction potential ($E^0_M = -1.90$ V versus SCE, compare Equation (64)), and during electrolysis it underwent a clearly observable deactivation, so that this particular mediator proved to be a very good candidate to test the validity and experimental worthiness of our above theoretical conclusions.

Figure 3a shows the variations of the catalyst concentration during two different electrolyses performed under identical conditions except for the modification of the electrolysis potential that can be observed to affect drastically the mediator deactivation rate. These results establish that in agreement with our above prediction [Eqs. (38–40)] a more negative cathode potential E results in a faster decomposition albeit the duration of experiment is shorter. Indeed, a less negative cathode potential E imposes a smaller $[M]^* = [M]^{bulk}/\{1+\exp[F(E-E^0_M)/RT]\}$ value so that both $[M]^*/[RX]^{bulk}$ and $\lambda_2 = k_{27}([M]^*/[(\delta^2/4D)$ are smaller. Figure 3b confirms that at a given value of the cathodic potential, the rate of decomposition of the catalyst is a fast decaying function of the organic halide excess factor $\gamma = [RX]^{bulk}/[M]^{bulk}$. In a usual batch electrolysis (data shown as open circles in Figure 3b) the rate of conversion of the organic halide is faster than the decomposition rate of the mediator and as consequence the instant γ value decreases while electrolysis

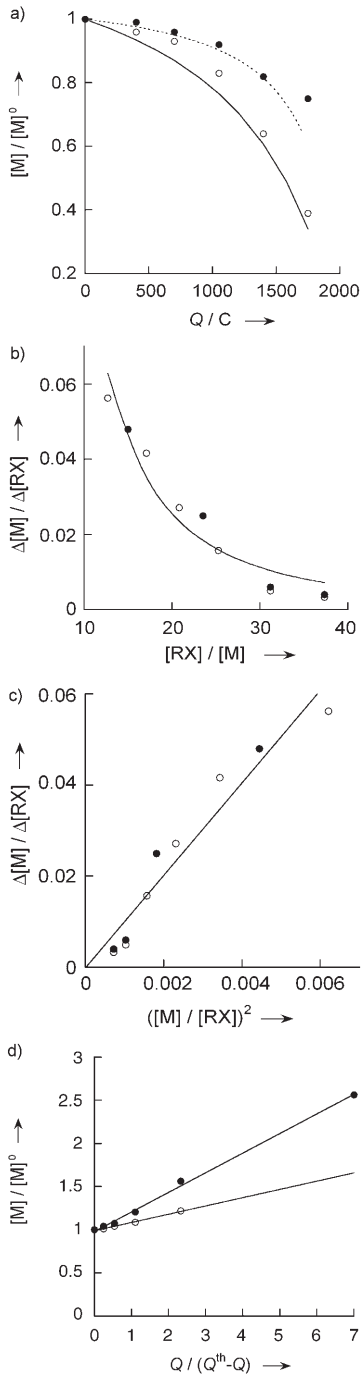

Figure 3. a) Influence of the charge consumed (C) on the catalyst decomposition: experimental data obtained at an electrolysis potential of $E = E^0 - 0.17$ V (○) or $E^0 + 0.015$ V (●), as compared to the corresponding theoretical predictions: $1/[1+0.277Q/(2000-Q)]$ (——) and $1/[1+0.096Q/(2000-Q)]$ (– – –). Initial RX concentration = 0.2 M; Initial catalyst concentration = 5 mM; SSE: NMP 0.1 M Bu_4NBr; CO_2 saturated, atm pressure ($[CO_2] = 0.14$ M). b) Influence of the ratio [RX]/[M] on the catalyst decomposition: experimental data at variable (○) and fixed (●) substrate concentration as compared to the corresponding theoretical predictions by expression in Equation (40) (——) obtained with a $\lambda/2$ of 10. Electrolysis potential of $E = E^0 - 0.17$ V. Initial catalyst concentration = 5 mM; SSE: NMP 0.1 M Bu_4NBr. CO_2 saturated, atm pressure ($[CO_2] = 0.14$ M). c) Plot of the same data as shown in Figure 3b as a function of $([M]/[RX])^2$, see Equation (40): Experimental data at variable (○) and fixed (●) substrate concentration, fitted data by Equation (40) (——) (slope 10.1; correlation coefficient 0.94). Electrolysis potential of $E = E^0 - 0.17$ V. Initial catalyst concentration = 5 mM; SSE: NMP 0.1 M Bu_4NBr; CO_2 saturated, atm pressure ($[CO_2] = 0.14$ M). d) Plot of the same data as shown in Figure 3a as a function of $Q/(Q^{th}-Q)$, see Equation (65): Electrolysis potential (●) $E \approx E^0 - 0.17$ V ($y = 0.23x + 0.98$; correlation coefficient: 0.997) and (○) $E \approx E^0 + 0.015$ V ($y = 0.096x + 0.99$; correlation coefficient: 0.993). Initial RX concentration = 0.2 M; initial catalyst concentration = 5 mM; SSE: NMP 0.1 M Bu_4NBr; CO_2 saturated, atm pressure ($[CO_2] = 0.14$ M).

proceeds leading to an increase of the rate of decomposition (as shown in Figure 3a). This effect may be compensated by additions of RX into the cell while electrolysis proceeds so that the excess factor γ is maintained constant at its initial value during electrolysis. Then the rate of mediator decomposition is found to be constant when electrolysis proceeds and depends only on the value of the excess factor γ (data shown as black circles in Figure 3b). Both series of data (Figure 3a and b) qualitatively support all the conclusions of our theoretical analysis.

In the following, we wish to examine if a similar good agreement exists at the quantitative level. In this respect, it must be recalled that our analysis was developed in order to predict how a perfect electrolysis starts to deviate from an ideal redox catalytic behavior. Therefore our Equations (38–40) are formally valid only for minimal deviations (that is, for $y_F \approx 1$). The data in Figure 3a and b involve much larger deviations concerning the losses of mediator per se, but they nevertheless correspond to Faradaic yields that approach unity. For example the maximum decomposition rate of catalyst in Figure 3b is at maximum 2% of the electrolysis rate (being 0.5 mol per F for RX as compared to 10 mmol per F for the mediator at $\gamma = 15$). Therefore even if the level of approximation used in developing our theoretical analysis is mathematically too low to be appropriate for a quantitative estimation of experimental data such as those in Figure 3a and b, they provide good guidelines to evaluate the theoretical significance of these experimental data.

Figure 3c presents the set of data shown in Figure 3b but re-plotted under the form of Equation (40). It is seen that the experimental data actually follow a linear variation with $([M]^*/[RX]^{bulk})^2$ as predicted by Equation (40), with a slope $\lambda/2$ of about 10 (where $[M]^* \rightarrow [M]^{bulk}$ since $E \ll E^0$).

Concerning the variations of the catalyst concentration during the electrolyses performed under exactly identical conditions except for the modification of the electrolysis potential, Equation (43) can be written as:

$$\frac{[M]^0}{[M]} \approx 1 + (\frac{\sigma}{2})(\frac{[M]^0}{[RX]^0})\frac{Q}{Q^{th}-Q} \qquad (65)$$

Figure 3d presents the two sets of data shown in Figure 3a but re-plotted by using Equation (65). We see that the experimental data follow a linear variation with $Q/(Q^{th}-Q)$ as predicted by Equation (65), with a higher slope for those obtained at the more negative cathode potential, thus reflecting that σ increases when E is made more negative. However, note that the agreement is not total due to the too small level of approximation used in the derivation. This is reflected by the fact that the value of the ratio $\lambda_{E=E^0+0.015\,V}/\lambda_{E=E^0-0.17\,V}$ computed by the slopes of Figure 3d, gives a ratio lower than unity when the opposite was expected according to Equations (43) and (66).

$$\lambda = \{k_{26} + {}^2/_3 k_{27}([M]^*\}(\frac{\delta^2}{4D}) \qquad (66)$$

We also note that very close values of $\lambda/2 \approx 10$ were estimated by fitting experimental data of the same synthesis respectively versus the ratio [RX]/[M] by Equation (40) and versus $Q/(Q^{th}-Q)$ by Equation (65).

There is therefore an extremely good agreement between the observed phenomena and all the trends predicted by the model developed above to evaluate the effect of a slow decomposition of the redox mediator occurring in parallel with the redox catalytic process (Scheme 2), especially when one takes into account that these theoretical predictions were elaborated only to examine how an efficient process departs from its ideal behavior, namely, should be restricted to conditions involving an extremely low consumption of the mediator. Under such ideal conditions, the variations of λ, as determined from the slopes of plots such as those presented in Figure 3c with the initial concentration of the catalyst, should allow us to investigate the exact nature of the catalyst decomposition reactions (Scheme 2). Indeed, the variation of λ versus $[M]^*$ should give the values of $k_{26}(\delta^2/D)$ and $k_{27}(\delta^2/D)$ by using Equation (66). This was not attempted because if the experimental trends are adequately followed, the magnitude of the slopes are inadequate, reflecting the too low level of approximation of the theoretical laws. Hence we preferred to investigate these kinetic aspects by a simple and more precise investigation by using cyclic voltammetry.

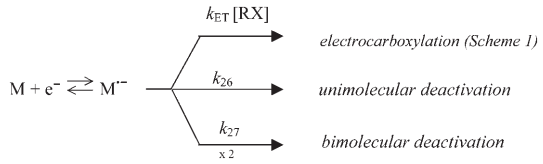

Scheme 2.

Validation of the above mechanistic conclusions by cyclic voltammetry: In the above section we derived some mechanistic conclusions based on the variations of the product yields or the redox mediator decomposition rate during preparative-scale electrolyses. We now examine the validity of the mechanistic schemes and elucidate them on the basis of an elementary investigation of the system by cyclic voltammetry.

Voltammograms and chronoamperograms were recorded by using vitreous carbon and platinum disc electrodes for solutions of 1,3-benzenedicarboxylic acid dimethyl ester at different concentrations (2–16 mM) in DMF/Bu_4NBr (0.1 M) both in the absence and in the presence of the substrate (1-phenyl-1-chloroethane). Chronoamperometric and voltammetric results were in good agreement with the reaction pathways depicted in Scheme 2. In fact, experimental results could be fitted satisfactorily, for all the range of concentrations investigated, with a reaction scheme where the radical anion decomposes by both a second-order ($k_{27} \approx 800\,M^{-1}\,s^{-1}$) and a first-order chemical reaction ($k_{26} \approx 1\,s^{-1}$). Hence, it is

possible to achieve, by using Equation (66) with $D = 10^{-5}\,cm^2s^{-1}$ and $\delta = 10^{-2}\,cm$, a rough estimation of $\lambda \approx 10$. Note, however, that the value of λ estimated by cyclic voltammetry is significantly lower than that (≈ 20) estimated by fitting experimental data by using Equation (66). On the other hand it should be observed that the kinetic constants mentioned above were estimated in an environment free of metallic cations while during the electrolysis a continuous release of aluminum cations was provided by the sacrificial anode. Indeed, we have recently observed (data not shown) that the presence of metallic cations in solution leads to a decrease of the stability of the radical anion of the catalyst (for example, an increase of the kinetic constants k_{26} and/or k_{27}). Hence, the observed difference may be attributed to the presence of aluminum cations in solution. Indeed, an electrolysis performed in the absence of sacrificial anodes in a divided cell with a constant excess factor of 40 gave rise to a $\Delta[M]^{bulk}/\Delta[RX]^{bulk}$ value of about 70% with respect to that observed with the same excess factor in an undivided cell in the presence of sacrificial anodes, and correspondingly, to a value of λ of about 14, closer to that estimated by electroanalytical experiments. Note that a difference still arises due to the too small level of approximation used.

According to Scheme 1, the 1-phenyl-1-chloroethane can itself be the proton donor that reacts with the corresponding anion R^- [Eqs. (51) and (55)]. Hence, electroanalytical experiments performed in the presence of the substrate should show the voltammetric peak due to styrene. However, the peak attributable to styrene occurs at a potential very similar to that arising from the direct reduction of 1-phenyl-1-chloroethane at a platinum cathode. Nevertheless, by reducing the 1-phenyl-1-chloroethane at a more positive potential, by homogeneous reduction, it was possible to observe a quasi-reversible peak having the same characteristic, in terms of peak potentials, to that of styrene (Figure 4a). According to Scheme 1, the presence of carbon dioxide and/or a proton donor should compete with the styrene formation.

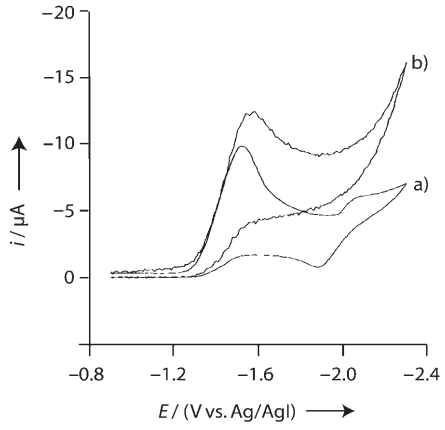

Figure 4. Cyclic voltammetry of 3-benzenedicarboxylic acid dimethyl ester (5 mM) in NMP-TBABr (0.1 M) and 1-phenyl-1-chloroethane (10 mM) in a) the absence and b) the presence of saturated carbon dioxide at a platinum electrode (1 mm radius) at scan rate 0.1 Vs^{-1}; reference $Ag/AgI/I^-$.

Hence, addition of one of these compounds to the solution should lead to a decrease of the peak attributed to the styrene. Indeed, when hydroquinone or carbon dioxide (Figure 4b) were added stepwise to the solution of 1,3-benzenedicarboxylic acid dimethyl ester (5 mM) and 1-phenyl-1-chloroethane (10 mM) in *N*-methyl-2-pyrrolidone (NMP), an increase of the catalytic peak and a decrease of the peak attributed to the styrene were observed.

Conclusion

We have elucidated the experimental conditions that optimize the performance of the process of carboxylation of benzyl halides catalyzed by homogeneous charge-transfer mediators in terms of both yield in the target carboxylic acid and minimization of the catalyst deactivation. In the catalyzed reaction, the carboxylation competes prevalently with the homogeneous reduction of the carbon dioxide and with the reaction of the benzylic anion with both the substrate and proton donors present in the solution. Since the yield of oxalate decreases upon increasing the value of $[RX]^{bulk}/[CO_2]$, while that of styrene increases with the same factor, the yield of carboxylate is a bell-shaped function of this ratio with a maximum that has been theoretically and experimentally determined. The competition between carbon dioxide and the substrate homogeneous reduction has also been confirmed theoretically to depend drastically on the redox standard potential of the mediator. A relationship that gives the optimum redox standard potential of the mediator has been evaluated that agrees with previous published experimental results. It has also been theoretically demonstrated that in a catalyzed process at a preparative-scale level, any slow catalyst decomposition reaction, although unnoticeable at the voltammetric level, can lead to a relevant deactivation of the catalyst. The theoretical dependence of the catalyst deactivation on operative parameters has been investigated. In particular the catalyst deactivation can be unexpectedly minimized by operating at a sufficiently high $[RX]^{bulk}/[catalyst]$ ratio. All the theoretical conclusions were confirmed experimentally in the case of the carboxylation of 1-phenyl-1-chloroethane catalyzed by 1,3-benzenedicarboxylic acid dimethyl ester and allowed the optimization of this tandem system.

Experimental Section

Electroanalytical procedure: The electroanalytical experiments were carried out in *N*,*N*-dimethylformamide (DMF) or *N*-methyl-2-pyrrolidone (NMP) with 0.1 M tetrabutylammonium bromide (Bu_4NBr) as the supporting electrolyte, a platinum or a vitreous graphite disc as the working electrode, a platinum spiral as the counter electrode, and SCE or $Ag/AgI/I^-$ 0.1 M in DMF as the reference electrode. Voltammetric scan and chronoamperometric measurements were performed by using an AMEL System 5000 potentiostat and Nicolet 3091 oscilloscope for data acquisition.

Electrosyntheses: Potentiostatic electrolyses were performed in undivided tank glass cells with planar geometry equipped with a gas inlet, an Ag/AgI/I^- 0.1 M DMF reference electrode, two 99.99% aluminum sacrificial anodes, and a graphite cathode. The volume of the solution was 50 mL.

Aluminum electrodes (surface 5 cm^2) were treated with 20% aqueous hydrochloric acid, then carefully washed with distilled water and acetone, and finally dried with nitrogen. The graphite working electrodes were washed with distilled water and acetone, then they were mechanically polished with sand paper, and treated by heating to a red color prior to use. The counter-electrode reaction was the anodic dissolution of the aluminum electrode. The electrolytic solution was stirred by a cylindrical Teflon-coated magnetic stir bar and by the continuous bubbling of carbon dioxide. Electrical power for preparative-scale experiments was supplied by an AMEL Model 533 potentiostat equipped with an AMEL Model 731 coulometer.

Workup of electrolytic solution: After electrolysis the solvent was evaporated under reduced pressure, the residue was acidified with aqueous hydrochloric acid, and was then extracted with diethyl ether. After evaporation of the solvent it was possible to recover the raw carboxylic acid that was crystallized in ethanol.

Main products were identified by comparison with commercial standards by using high-performance liquid chromatography (HPLC). Product structures were confirmed by making NMR and GC-MS measurements. Periodical analyses of the electrolytic solution were performed during the electrosyntheses by removing samples of 2 cm^3 volume from the cell. An HPLC instrument (Perkin–Elmer 410 LC) equipped with a UV detector and Supelco LC8 and LC18 columns was employed. The eluent was a mixture of MeCN and water, acidified with CH_3COOH. GC–MS analyses were carried out by using a Perkin–Elmer Turbomass and Autosystem XL chromatograph equipped with a SGE capillary column.

Chemicals: DMF and NMP anhydroscan-grade solvents from Labscan (max water content 100 ppm) were used which were further dried with molecular sieve 4 Å. The ammonium salt Bu_4NBr was crystallized twice from ethyl acetate. 1-Phenyl-1-chloroethane was analytical grade (Aldrich).

Acknowledgements

This work was supported in part by CNRS and Ecole Normale Superieure in Paris, and by the Ministero dell'Istruzione, dell'Università e della Ricerca (MIUR) and the University of Palermo.

[1] M. M. Baizer, J. L. Chruma, *J. Org. Chem.* **1972**, *37*, 1951.
[2] D. A. Koch, B. J. Henne, D. E. Bartak, *J. Electrochem. Soc.* **1987**, *134*, 3062.
[3] G. Silvestri, S. Gambino, G. Filardo, A. Gulotta, *Angew. Chem.* **1984**, *96*, 978; *Angew Chem. Int. Ed. Engl.* **1984**, *23*, 979.
[4] O. Sock, M. Troupel, J. Perichon, *Tetrahedron Lett.* **1985**, *26*, 1509.
[5] G. Silvestri, S. Gambino, G. Filardo, *Enzymatic and Model Carboxylation and Reduction Reactions for Carbon Dioxide Utilisation*, Kluwer Academic Publishers, The Netherlands, **1990**, pp. 101–127, and references therein.
[6] J. Chaussard in *Electrosyntheses From Laboratory, to Pilot, to Production* (Eds.: J. D. Genders, D. Pletcher), The Electrosynthesis Company Inc., New York, **1990**, Chapter 8.
[7] O. Scialdone, G. Filardo, A. Galia, G. Silvestri, *Acta Chem. Scand.* **1999**, *53*, 800.
[8] O. Scialdone, C. Belfiore, G. Filardo, A. Galia, G. Silvestri, *Ind. Eng. Chem. Res.* **2004**, *43*, 5006.
[9] J. F. Fauvarque, A. Jutand, M. Francois, *J. Appl. Electrochem.* **1988**, *18*, 109.
[10] J. F. Fauvarque, A. Jutand, M. Francois, M. A. Petit, *J. Appl. Electrochem.* **1988**, *18*, 109.
[11] C. Amatore, A. Jutand, *Organometallics* **1988**, *7*, 2203.
[12] C. Amatore, A. Jutand, *J. Am. Chem. Soc.* **1991**, *113*, 2819.
[13] S. Torii, H. Tanaka, T. Hamatani, K. Morisaki, A. Jutand, F. Pfluger, J. F. Fauvarque, *Chem. Lett.* **1986** 169.
[14] C. Amatore, A. Jutand, F. Khalil, M. F. Nielsen, *J. Am. Chem. Soc.* **1992**, *114*, 7076.
[15] A. Gennaro, A. A. Isse, F. Maran, *J. Electroanal. Chem.* **2001**, *507*, 124.
[16] A. A. Isse, M. G. Ferlin, A. Gennaro, *J. Electroanal. Chem.* **2003**, *541*, 93.
[17] A. A. Isse, A. Gennaro, *Chem. Commun.* **2002**, 2798.
[18] A. A. Isse, M. G. Ferlin, A. Gennaro, *J. Electroanal. Chem.* **2005**, *581*, 2798.
[19] G. Silvestri, S. Gambino, G. Filardo, *Acta Chem. Scand.* **1991**, *45*, 987.
[20] A. Gennaro, A. A. Isse, J. M. Saveant, M. G. Severino, E. Vianello, *J. Am. Chem. Soc.* **1996**, *118*, 7190.
[21] C. Amatore, C. Pebay, O. Scialdone, S. Szunerits, L. Thouin, *Chem. Eur. J.* **2001**, *7*, 2933.
[22] J. Simonet, M. A. Michel, H. Lund, *Acta Chem. Scand.* **1975**, *B29*, 489.
[23] H. Lund, J. Simonet, *J. Electroanal. Chem.* **1975**, *65*, 205.
[24] H. Lund, K. Daasbjerg, D. Occhialini, S. U. Pedersen, *Russ. J. Electrochem.* **1995**, *31*, 939.

Received: December 1, 2005
Revised: March 1, 2006
Published online: July 19, 2006

